Selectivity Control for the Catalytic 1,3-Butadiene Hydrogenation on Pt(111) and Pd(111) Surfaces: Radical versus Closed-Shell Intermediates

Ana Valcárcel,[†,‡] Anna Clotet,[†] Josep M. Ricart,[†] Françoise Delbecq,[*,‡] and Philippe Sautet[‡]

Departament de Química Física i Inorgànica, Universitat Rovira i Virgili, Marcel·lí Domingo s/n, E-43007 Tarragona, Spain, and Laboratoire de Chimie, UMR CNRS 5182, Ecole Normale Supérieure de Lyon, 46 Allée d'Italie, F-69364 Lyon Cedex 07, France

Received: April 22, 2005; In Final Form: May 27, 2005

The hydrogenation of 1,3-butadiene to different C_4H_8 species on both Pd(111) and Pt(111) surfaces has been studied by means of periodic slabs and DFT. We report the adsorption structures for the various mono- and dihydrogenated butadiene intermediates adsorbed on both metal surfaces. Radical species are more clearly stabilized on Pt than on Pd. The different pathways leading to these radicals have been investigated and compared to those producing 1-butene and 2-butene species. On palladium, the formation of butenes seems to be clearly favored, in agreement with the high selectivity to butenes observed experimentally. In contrast, the formation of dihydrogenated radical species seems to be competitive with that of butenes on platinum, which could explain its poorer selectivity to butenes and the formation of butane as a primary product.

Introduction

The production of high-purity butene streams for polymerization or copolymerization processes requires the hydrogenation of the butadiene impurities contained in the butene cuts. The hydrogenation of 1,3-butadiene can lead to different products: partial hydrogenation yields butene, while total hydrogenation leads to butane. As the target product is the alkene, the catalyst must not hydrogenate any of the butene molecules and reduce the diolefine to butene rather than butane. The control over the selectivity of this catalytic reaction is then the crucial step. The active components of the catalysts are usually noble metals, such as palladium or platinum. Palladium is still considered as the best catalyst for partial hydrogenation of alkadienes.[1] Exhaustive experimental studies on single-crystal catalytic surfaces have shown that a selectivity approaching 100% for the partially hydrogenated product (mainly 1-butene) is obtained in the case of Pd(111), while Pt(111) is much less selective (only 60%).[2−7] The difference between the reaction on palladium and platinum surfaces has been previously ascribed to both the different adsorption strength and adsorption modes of 1,3-butadiene and butenes.[8−11] The strongly adsorbed 1,3-butadiene displaces the more weakly adsorbed butenes from the Pd(111) surface. Then, no further hydrogenation can occur. On the other hand, on the Pt(111) face, it has been proposed from semiempirical calculations[11] that the adsorption strength of 1,3-butadiene is equivalent to that of butene. Therefore, a lower selectivity is expected. Similar arguments have been invoked to explain the high selectivity of the Pd catalyst on the hydrogenation of acetylene.[12] However, a later study[13] has pointed out that these arguments are not complete, as they cannot explain the noticeable ethylene hydrogenation observed under high pressures of acetylene. Moreover, these adsorption competition arguments do not take into account the presence of other intermediate species on the surface.

Toward a deeper understanding of the different surface reactivity for 1,3-butadiene on Pd(111) and Pt(111) surfaces, we have carried out a comparative DFT study of the adsorption of 1,3-butadiene and butenes on these metallic surfaces.[14] The energy difference between the most stable adsorption modes for 1,3-butadiene and 1-butene has been found to be 67 kJ mol^{-1} on Pt(111) vs 79 kJ mol^{-1} on Pd(111), butadiene being the most stable species. Therefore, it is difficult to attribute the different selectivity observed to this slight tendency of Pd to give a more facile butene desorption by competition with butadiene adsorption. It is not clear indeed why Pt cannot give the same result. Moreover, early experimental studies[15] have shown that butane is a direct product for 1,3-butadiene hydrogenation on Pt, in contrast to palladium, where the initial formation of butane is negligible. Additionally, several papers have dealt with the reactivity of metallacyclic intermediates, which can play quite an important role in hydrogenation−dehydrogenation reactions.[16−18] Consequently, to answer the problem of the selectivity, it seems to be necessary to go further in the detailed description of the hydrogenation reaction itself.

In this paper, we investigated the hydrogenation of 1,3-butadiene to different C_4H_8 species on both Pd(111) and Pt(111) surfaces by means of density functional theory (DFT). The objective of this study was twofold: to determine the adsorption structures for the various mono- and dihydrogenated butadiene moieties and to investigate and compare the competitive reaction pathways in order to unravel the origin of the catalytic selectivity. We analyzed the reaction pathways and energetics for the hydrogenation on the basis of the Horiuti−Polanyi mechanism.[19]

Computational Methods and Systems

The calculations were performed in the framework of DFT using the Vienna Ab Initio Simulation Program (VASP).[20−22] This program solves the Kohn−Sham equations of the density functional theory with the development of the one-electron wave function in a basis of plane waves. The electron−ion interactions were described by the projector augmented wave method (PAW) introduced by Blöchl[23] and adapted by Kresse and Joubert.[24] A tight convergence of the plane-wave expansion was obtained with a cutoff of 400 eV. The exchange−correlation energy and

* To whom correspondence should be addressed.
† Universitat Rovira i Virgili.
‡ UMR CNRS 5182, Ecole Normale Supérieure de Lyon.

10.1021/jp052087m CCC: $30.25
Published on Web 07/01/2005

potential were described by the generalized gradient approximation (Perdew−Wang 91).[25] The 2D Brillouin zone integrations were performed on a 3 × 3 × 1 Monkhorst-Pack grid, as it was found to be accurate as well as computationally efficient.[14]

The Pt(111) and Pd(111) surfaces were modeled by the repeated slab approach; an infinite two-dimensional slab in a three-dimensional periodic cell is generated by introducing a sufficiently large vacuum width in the direction perpendicular to the surface (∼12 Å). The metal slabs were chosen to be four layers thick. In previous studies,[14,26] some tests have been performed to investigate the effect of the slab thickness on the computed energies. The comparison between four-layer and six-layer slabs has shown us that the results are consistent only when the k-point convergence is reached (the six-layer model needing a larger grid) and that the four-layer slab is an adequate model. The Pt−Pt and Pd−Pd interatomic distances have been optimized to 2.82 and 2.80 Å for the bulk, which are very close to the experimental values 2.77 and 2.75 Å.[27] In this study, 3 × 3 super-cells were used. Adsorption and reaction were performed on one side of the metal slab. The geometries of the two uppermost layers of the surface together with the adsorbate (C_4H_x, $x = 6-8$ species) were fully optimized, whereas the two lowest metal planes were kept fixed at the optimized bulk geometry. The adsorption modes and the corresponding adsorption energies for all the C_4H_x moieties were determined. Reaction intermediates were studied on different adsorption sites. For the sake of simplicity, only the stable structures are reported here. Coadsorption with hydrogen was also explored in detail by comparing various possible situations.

The energy along the reaction (E_{React}) was calculated using butadiene and H_2 in the gas phase as the energy reference with the following expression:

$$E_{Re\boldsymbol{act}} = E_{syst/surface} - E_{surface} - E_{C_4H_{6(g)}} - E_{H_{2(g)}}$$

A negative value indicates an exothermic chemisorption process. The system is a C_4H_x species and $(8 - x)$ hydrogen atoms ($x = 6, 7, 8$) adsorbed on the surface. If we consider that the hydrogen atoms and the hydrocarbon do not interact, the $E_{syst/surface}$ term is then obtained by combining the results from independent slab calculations for the molecular species and the hydrogen atoms:

$$E_{syst/surface} = E_{C_4H_x/surface} + (8 - x)(E_{H/surface} - E_{surface})$$

For butadiene the calculation of the adsorption energy has already been done,[14] and for the H atom we found here that the most stable adsorption site is fcc hollow with an adsorption energy of −48 kJ mol^{-1} on Pt and −67 kJ mol^{-1} on Pd. For the final product butene, E_{React} is the sum of the butene adsorption energy[14] and the reaction energy in the gas phase (butadiene + H_2 → butene, $\Delta E_{React} = -136$ and −152 kJ mol^{-1} for 1-butene and 2-butene, respectively).

To directly compare with previous results, the adsorption energy for the species existing in the gas phase has also been reported ($E_{ads} = E_{C_4H_x/surf} - E_{surface} - E_{C_4H_x}$ ($x = 6, 8$)). This allows a better understanding of the contribution of C_4H_x and hydrogen in the comparison of E_{React} values for the two metals. For the sake of simplicity, the energies of the transition states (E_{TS}) were calculated with respect to adsorbed butadiene and two adsorbed hydrogen atoms without interaction (Figures 2 and 4).

The nudged elastic band method (NEB)[28] in combination with the dimer method,[29] both developed by Jónsson and co-workers,

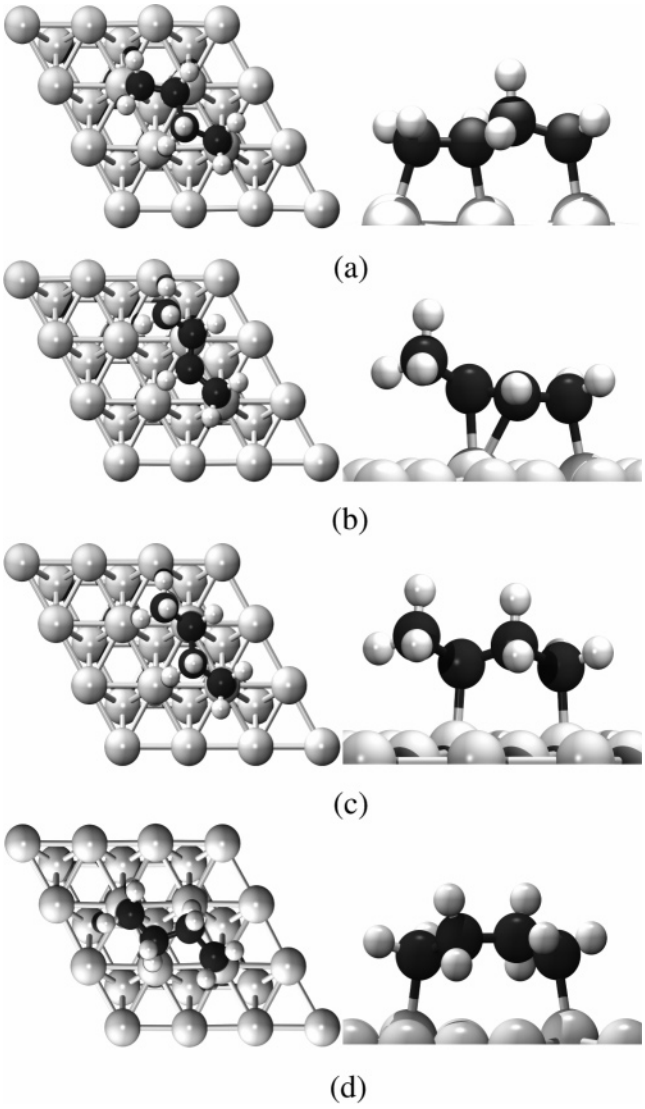

Figure 1. Adsorption modes for 1-buten-4-yl (1B4R, a), 2-buten-1-yl (2B1R,b), butan-1,3-diyl (B13R, c), and butan-1,4-diyl (B14R, d) on Pd and Pt (111) metal surfaces.

were used to determine the transition states. First, a set of images (8) between the initial (reactants) and final (products) states were obtained by linear interpolation. In the NEB method, each image is optimized in a hyperspace perpendicular to the reaction path direction, locally defined as the direction between two subsequent images. The minimization of the forces acting on the images would bring the NEB to the minimum energy path (MEP). After a few iterations, a rough estimate of the shape of the MEP was obtained. Then, the two images with higher energy were chosen to be the starting point for the dimer method. The "dimer" (two images separated by a fixed distance from a central point) is formed from the two selected replicas of the system. The dimer is rotated keeping its center fixed in order to minimize the potential energy (identifying the lowest curvature direction). Then, the forces acting on the center of the dimer are calculated, and a so-called "effective force" is defined as the opposite of the component along the dimer. Minimization with respect to this effective force moves the dimer to the saddle point. The results obtained were refined until a negligible value of the forces with the quasi-Newton algorithm implemented in VASP. This sequence of algorithms (NEB, DIMER, quasi-Newton) was indeed found to be the most efficient for the transition state search.

SCHEME 1: 1,3-Butadiene Hydrogenation to C_4H_8 Species via the Horiuti−Polanyi Mechanism

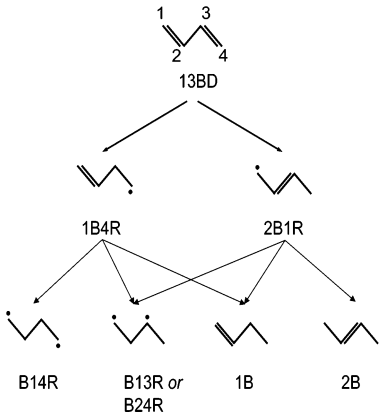

To validate the saddle points obtained, we performed a full vibrational analysis. We checked cautiously that all the structures obtained have a single imaginary frequency and the corresponding mode is consistent with the reaction path studied. Zero point energy (ZPE) corrections were not considered in the calculation of activation barriers, but their influence was evaluated. Test calculations on two of our target systems showed that the ZPE contribution to the activation energy was smaller than 1−2 kJ mol^{-1} on both metal surfaces. Moreover, no changes in the relative energies of the transition states (E_{TS}) were found.

Results

Binding of the C_4H_x ($x = 7, 8$) Radical Species. Scheme 1 summarizes the network of steps by which 1,3-butadiene can be dihydrogenated to a C_4H_8 species. In an earlier paper,[14] we have studied the adsorption modes and adsorption energies of 1,3-butadiene (CH_2═$CHCH$═CH_2, 13BD), 1-butene (CH_3CH_2CH═CH_2, 1B), and 2-butene (CH_3CH═$CHCH_3$, 2B) on both Pt(111) and Pd(111) surfaces.

For these species, the adsorption energies (E_{ads}) and the outstanding structural parameters are reported in Table 1 along with E_{React}, since this information is crucial in analyzing the hydrogenation reaction pathways. The difference of E_{React} for 1,3-butadiene on Pt and Pd can hence be related to the different adsorption energy for H on these metals. It has been determined that the most stable adsorption mode for 1,3-butadiene is the 1,2,3,4-tetra-σ one (the molecule is adsorbed in its *trans* form and interacts with the metal surface via its four C atoms) on both metal surfaces with a very similar adsorption energy. Although other structures lie in a small range of energies, we considered only the reaction pathways starting from the most stable one. This is not a real limitation, as the molecule can readapt its geometry prior to hydrogenation during the pathway optimization. The Horiuti−Polanyi mechanism (see Scheme 1) implies the initial formation of a C_4H_7 moiety and the subsequent hydrogenation to a C_4H_8 species. Addition of the first hydrogen atom produces only two different intermediate radicals because the 1,3-butadiene molecule in the *trans* form belongs to the C_{2h} point group. The H-addition on the C_3 (or C_2) atom produces the 1-buten-4-yl radical CH_2═$CHCH_2CH_2^{\bullet}$ (1B4R), and the H-addition on C_4 (or C_1) produces the 2-buten-1-yl radical $CH_2^{\bullet}CH$═$CHCH_3$ (2B1R). For the sake of simplicity, the nomenclature used here follows the IUPAC conventions for gas phase radicals. In the abbreviated nomenclature (in parentheses), the first number accounts for the position of the "remaining" double bond and the second one accounts for the number of the radical C atom, R simply indicating that the fragment is a radical in the gas phase. For both radicals (1B4R and 2B1R), there are three possibilities to add a second hydrogen atom. For 1-buten-4-yl, the addition on C_1 produces the butan-2,4-diyl diradical $CH_3CH^{\bullet}CH_2CH_2^{\bullet}$ (B24R), on C_2 the butan-1,4-diyl diradical $CH_2^{\bullet}CH_2CH_2CH_2^{\bullet}$ (B14R), and on C_4 the 1-butene species. The 2-buten-1-yl radical gives 2-butene, butan-1,3-diyl $CH_2^{\bullet}CH_2CH^{\bullet}CH_3$ (B13R), and 1-butene from C_1, C_2, and C_3 hydrogenation, respectively. Although obtained through two different paths, the butan-2,4-diyl and the butan-1,3-diyl species are strictly equivalent. We will name this moiety butan-1,3-diyl (B13R) according to the current nomenclature.

Figure 1 shows the most stable adsorption modes for 1-buten-4-yl, 2-buten-1-yl, butan-1,3-diyl, and butan-1,4-diyl radicals, which are similar on both metal surfaces. These structures can be characterized as 1,2,4-tri-σ (Figure 1a), 1-σ-2,3-π (Figure 1b), 1,3-di-σ (Figure 1c), and 1,4-di-σ (Figure 1d). Both diradicals form a so-called metallacycle. This adsorption structure is common for dihaloalkanes of general formula $CH_3CHX(CH_2)_nCH_2X$ ($n = 1, 2$) dissociatively adsorbed in ultrahigh vacuum.[16−18] The most relevant geometrical parameters and the relative reaction energies (E_{React}) are presented in Table 1.

The Pt(111) surface stabilizes the radical species more than the Pd one does; that is, the adsorption energies are higher on Pt(111) than on Pd(111). This is especially true for the nonconjugated radicals. However, the trends are similar on both metal surfaces. The most stable species is the conjugated 2-buten-1-yl intermediate followed by the 1-buten-4-yl, and finally by the butan-1,3-diyl and the butan-1,4-diyl diradicals (see Scheme 2). It is important to note that the 2-buten-1-yl is stabilized by 42 kJ mol^{-1} with respect to the 1-buten-4-yl on the Pd surface, while the difference is only 17 kJ mol^{-1} on Pt(111). The diradical species are much less stable than the monoradical moieties on Pd(111) (>80 kJ mol^{-1}), while the difference is much smaller on the Pt(111) surface, where the best diradical is only 23 kJ mol^{-1} less stable than 2-buten-1-yl. However, we should take into account that this difference also includes the difference in adsorption energy of the hydrogen atom on these metals (−48 kJ mol^{-1} on Pt vs −67 kJ mol^{-1} on Pd). This difference (∼20 kJ mol^{-1}) helps us to explain the marked gap between C_4H_6 and the mono- and dihydrogenated species found on Pd(111) (see Scheme 2). As our aim is to study the hydrogenation of 1,3-butadiene to the different C_4H_8 species, it is especially relevant to compare the energy of the diradicals to that of the butene molecules (e.g., 1-butene). The butan-1,3-diyl radical is only 11 kJ mol^{-1} less stable than 1-butene on platinum, while on palladium the difference is 41 kJ mol^{-1}. The energy difference increases dramatically if one considers the 1,4-diradical (up to 71 kJ mol^{-1} on Pd). We will therefore not consider the butan-1,4-diyl in the study of the possible reaction pathways.

The adsorption geometries of the radical intermediates follow the same trends as those of 1,3-butadiene and butenes.[14] In general, there is no remarkable difference in the metal−carbon (M−C) and C−C bond distances obtained on both metal surfaces except for C−C bonds that directly interact with the metal surface of the monoradical species. In fact, the C_1-C_2 bond of the 1-buten-4-yl molecule is 1.45 Å on Pd, to be compared to the 1.49 Å value obtained on Pt. This result was also found for 1,3-butadiene in its di-σ adsorption mode.[14] Moreover, the C_1-C_2 bond of the 2-buten-1-yl intermediate is also shorter on Pd than on Pt, and, more important, the difference between the C_1-C_2 and the C_2-C_3 bonds is smaller in Pd than in Pt, which indicates a more allylic adsorption mode. The allylic

TABLE 1: Energy along the Reaction (E_{React}, kJ mol^{-1}), Adsorption Energy (E_{ads}, kJ mol^{-1}), and Relevant Geometrical Parameters (metal−carbon, M−C, and carbon−carbon, C−C, distances in Å) for the Different C_4H_x ($x = 6-8$) Species Adsorbed on Pt(111) and Pd(111)

system	E_{React}	E_{ads}	M−C_1	M−C_2	M−C_3	M−C_4	C_1−C_2	C_2−C_3	C_3−C_4
Pt(111)									
1,3-butadiene	−259	−163	2.10	2.18	2.18	2.11	1.48	1.48	1.48
1-buten-4-yl	−227		2.13	2.14		2.10	1.49	1.52	1.52
2-buten-1-yl	−244		2.10	2.33	2.19		1.46	1.42	1.50
butan-1,3-diyl	−221		2.09		2.12		1.52	1.52	1.52
butan-1,4-diyl	−176		2.11			2.11	1.53	1.54	1.53
1-butene	−232	−96	2.12	2.14			1.49	1.52	1.54
2-butene	−233	−81		2.13	2.13		1.52	1.50	1.52
Pd(111)									
1,3-butadiene	−297	−163	2.12	2.23	2.25	2.11	1.45	1.45	1.45
1-buten-4-yl	−220		2.14	2.15		2.07	1.45	1.52	1.52
2-buten-1-yl	−262		2.10	2.34	2.17		1.44	1.42	1.50
butan-1,3-diyl	−182		2.07		2.10		1.51	1.51	1.51
butan-1,4-diyl	−152		2.09			2.09	1.52	1.54	1.52
1-butene	−223	−87	2.13	2.14			1.45	1.52	1.54
2-butene	−220	−68		2.14	2.14		1.52	1.46	1.52

SCHEME 2: Energies (E_{React}) of the C_4H_x ($x = 6-8$) Species on Pt(111) and Pd(111) Surfaces

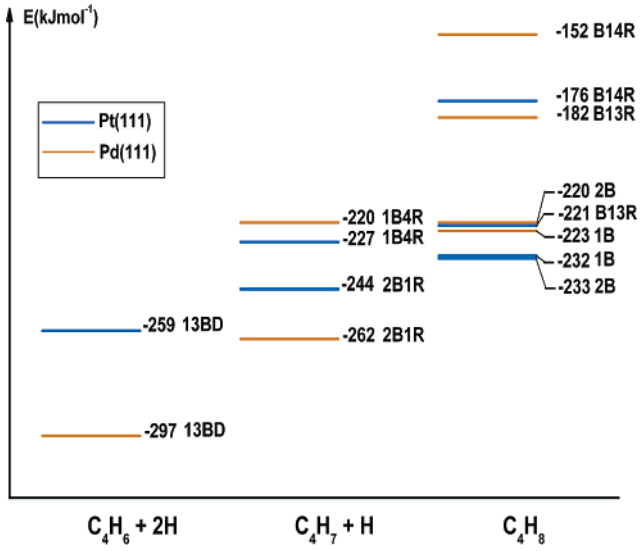

character of the adsorption structure could be responsible for the extra stabilization observed for the 2-buten-1-yl radical on Pd (see the above discussion about adsorption energies). All the C−C distances in the diradical species are within the range 1.51−1.54 Å. Clearly, all the C atoms have sp^3 hybridization. No significant differences are observed for the C−H distances (∼1.10 Å), except for the C_3−H and C_4−H bonds of the butan-1,4-radical directly pointing to metal surface (1.13 Å). This value suggests that these bonds are slightly activated due to the interaction with the metal surface (the M−H distance is indeed about 2.12 Å).

Coadsorption of C_4H_x ($x = 6, 7$) Species and Hydrogen. The next step toward understanding the hydrogenation of 1,3-butadiene was to examine the interaction between the hydrocarbon and the hydrogen atom. To account for lateral interactions between adsorbates on the metal surface, the hydrocarbon and one atomic H were coadsorbed in adjacent adsorption sites: the C_4H_x species was placed in its more stable adsorption site and hydrogen in a neighboring 3-fold hollow site close to the C atom to be hydrogenated. Several positions were tested, and the most stable ones were used as initial configurations for the reaction pathway searches. On coadsorption, there were no significant changes in the geometry of the C_4H_x moiety. Nevertheless, the picture for the H atom is rather different on the two metal surfaces. On palladium, all the positions surrounding the organic molecule were stable. On the other hand, in the case of platinum, the adsorbed hydrogen atom moved from the 3-fold hollow site closest to the hydrocarbon moiety (the H atom and the C_4H_x species share at least one of the surface metal atoms) to a quasi bridge position (one of the metal−hydrogen bonds is elongated by about 0.15 Å) or to a neighboring hollow site moving away from the C_4H_x intermediate. This is a consequence of the well-known high mobility of H atoms on both metal surfaces.[30] The calculated lateral interactions are not negligible (around 15−30 kJ mol^{-1}). These results are very similar to those obtained for ethylene[31] and acetylene[32] hydrogenation.

Reaction Pathways and Activation Barriers. Figure 2 shows the reaction pathways starting from the reactant (C_4H_6) to give the partial hydrogenation product species (C_4H_8) on the Pt(111) surface. The reference line (zero level) is the energy of the adsorbed 1,3-butadiene and two adsorbed hydrogen atoms at infinite distance (without interaction).

Geometries of the determined transition states are shown in Figure 3a−g. In all cases the basic structure of the activated complex is a three-center Pt−C−H unit. Whereas the C−H bond is formed, both the Pt−H and Pt−C bonds are broken. Somehow, the C═C bond is inserted into the Pt−H bond, as known in the case of hydrogenation by organometallic complexes.[33] Obviously, the Pt−C, C−H, and Pt−H bond distances characterize the activated complex (see Table 2). Generally, the shorter the C−H distance, the later the transition state.

As explained in section 3.1, the first hydrogenation can lead to two C_4H_7 intermediates: 1-buten-4-yl and 2-buten-1-yl. The corresponding TSs are depicted in Figure 3a,b. For the hydrogenation of 1,3-butadiene to 1-buten-4-yl, the computed TS energy is 97 kJ mol^{-1} (see Figure 2a), and the reaction barrier measured from the coadsorbed reactants is 80 kJ mol^{-1} (intrinsic barrier). The calculated energy for the saddle point leading to the 2-buten-1-yl radical is again 97 kJ mol^{-1}, with an intrinsic activation barrier of 81 kJ mol^{-1} (see Figure 2b). No preference for one of the possible "first steps" can be inferred from these results.

The second hydrogenation is more complex. From the 1-buten-4-yl intermediate, butan-1,3-diyl radical and 1-butene species can be obtained. The energy of the activated complex leading to the butan-1,3-diyl (Figure 3c) is 125 and 82 kJ mol^{-1} from the coadsorbed state. The TS connecting 1-buten-4-yl to 1-butene is shown in Figure 3d. This transition state is only 5 kJ mol^{-1} more stable than the one toward the diradical (120 vs 125 kJ mol^{-1}). Therefore, both reaction pathways may

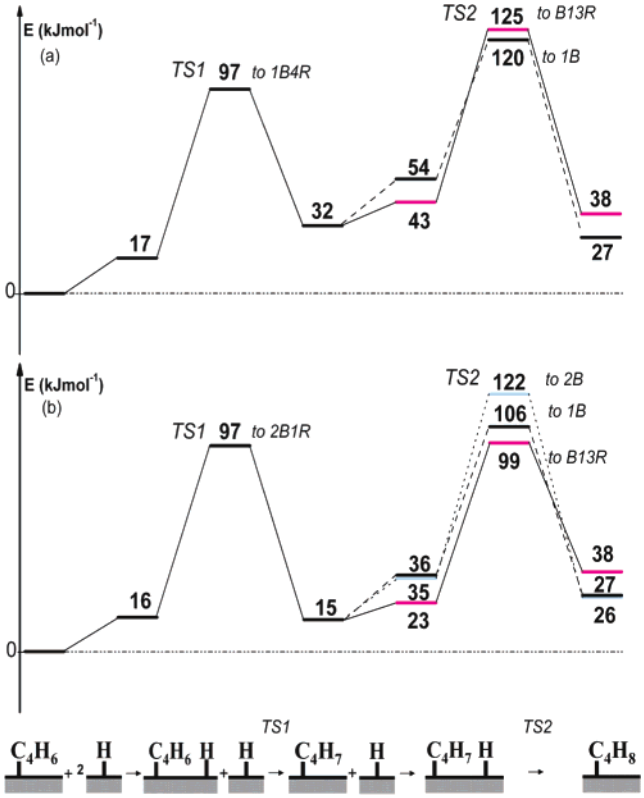

Figure 2. Butadiene hydrogenation energy profile on the Pt(111) surface via 1-buten-4-yl (1B4R, a) and 2-buten-1-yl (2B1R, b) intermediates. For the sake of clarity, the second hydrogenation step is drawn in a different color depending on the final product: butan-1, 3-diyl radical (pink), 1-butene (black), and 2-butene (light blue).

be competitive. The picture for the second hydrogenation from the 2-buten-1-yl radical has strong similarities with the one from 1-buten-4-yl. From 2-buten-1-yl, three different products can be obtained: 2-butene, butan-1,3-diyl, and 1-butene. For 2-butene (see Figure 3e), the energy of the TS is 122 kJ mol^{-1}. If one considers the barrier from the reactant state, this value decreases by 35 kJ mol^{-1}. For butan-1,3-diyl (Figure 3f) the energy of the saddle point is 99 kJ mol^{-1} (intrinsic barrier: 76 kJ mol^{-1}). Finally, the energy of the transition state leading to 1-butene (Figure 3g) is 106 kJ mol^{-1} above the zero level or 70 kJ mol^{-1} with respect to the reactant state.

A clear trend emerges from the structure of the transition states. TSs leading from a radical to a closed-shell fragment are late, with a short C−H bond (1.42−1.49 Å) and an already broken Pt−H bond (1.64−1.93 Å). The C−H bond formation process stabilizes the radical fragment, and overall this step is exothermic or neutral. On the other hand, transitions from closed-shell fragments to radicals are early and endothermic, although this effect is reduced for the formation of 2-buten-1-yl since the radical is stabilized by conjugation. Radical to diradical transition states are intermediate.

From these results we can conclude that no surface reaction pathway is clearly favored on Pt(111). The hydrogenation may take place via both the 1-buten-4-yl and the 2-buten-1-yl intermediates. Similar energies were also found for all second hydrogenation transition states, the differences being smaller than 26 kJ mol^{-1}. In the case of the pathways leading to butenes, the TS energies are consistent with a predominant formation of 1-butene (106 and 122 kJ mol^{-1} for the formation of 1-butene and 2-butene, respectively). Notice that only the pathways leading to *trans*-2-butene were computed. Experimentally both *trans*- and *cis*-2-butene are obtained in almost equal quantities,

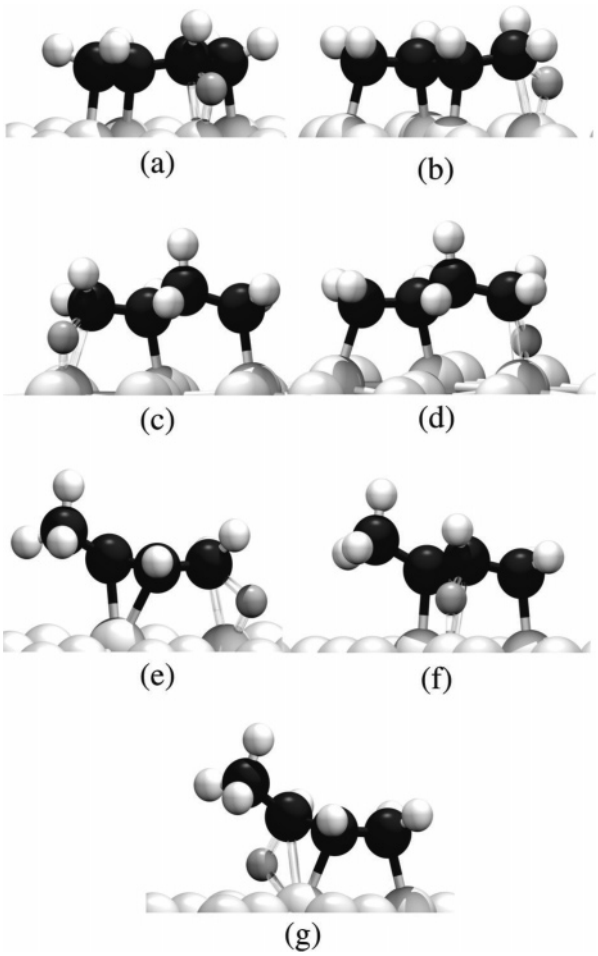

Figure 3. Transition state structures for the 1,3-butadiene hydrogenation on Pt(111): 13BD to 1B4R (a), 13BD to 2B1R (b), 1B4R to B13R (c), 1B4R to 1B (d), 2B1R to 2B (e), 2B1R to B13R (f), 2B1R to 1B(g). The reactive H atom is drawn in gray.

TABLE 2: Energy (E_{TS}, kJ mol^{-1}) and the Most Outstanding Structural Parameters (metal−hydrogen, M−H, carbon−hydrogen, C−H, and metal−carbon, M−C, distances in Å) of the Transition States for 1,3-Butadiene Hydrogenation on Pt(111) and Pd(111)

transition state	E_{TS}	M−H	C−H	M−C
Pt(111)				
1,3-butadiene → 1-buten-4-yl	97	1.60	1.65	2.42
1,3-butadiene → 2-buten-1-yl	97	1.61	1.57	2.28
1-buten-4-yl → butan-1,3-diyl	125	1.61	1.60	2.32
1-buten-4-yl → 1-butene	120	1.64	1.49	2.30
2-buten-1-yl → 2-butene	122	1.65	1.49	2.27
2-buten-1-yl → butan-1,3-diyl	99	1.63	1.62	3.04
2-buten-1-yl → 1-butene	106	1.93	1.42	2.46
Pd(111)				
1,3-butadiene → 1-buten-4-yl	132	1.61	1.57	2.38
1,3-butadiene → 2-buten-1-yl	96	1.73	1.50	2.31
1-buten-4-yl → butan-1,3-diyl	175	1.72	1.52	2.34
1-buten-4-yl → 1-butene	155	1.71	1.57	2.24
2-buten-1-yl → 2-butene	134	1.75	1.49	2.31
2-buten-1-yl → butan-1,3-diyl	159	1.72	1.40	3.06
2-buten-1-yl → 1-butene	120	1.81	1.46	2.36

and the relative amount of the two isomers depends on the reaction conditions.[5,7] One could assume that the hydrogenation pathways leading to the *cis* isomer are very similar to those described above. Moreover, butene isomers are not the only surface species possible in the 1,3-butadiene hydrogenation, but the butan-1,3-diyl radical can also be formed by a low-energy pathway. In fact, the saddle point leading to butan-1,3-diyl from

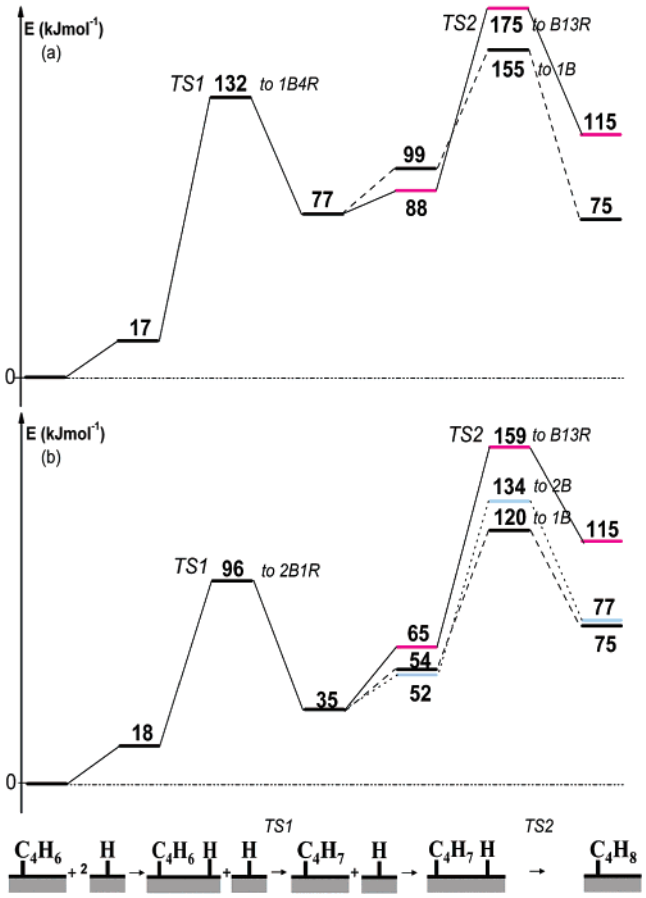

Figure 4. Butadiene hydrogenation energy profile on the Pd(111) surface via 1-buten-4-yl (1B4R, a) and 2-buten-1-yl (2B1R, b) intermediates. For the sake of clarity, the second hydrogenation step is drawn in a different color depending on the final product: butan-1, 3-diyl radical (pink), 1-butene (black), and 2-butene (light blue).

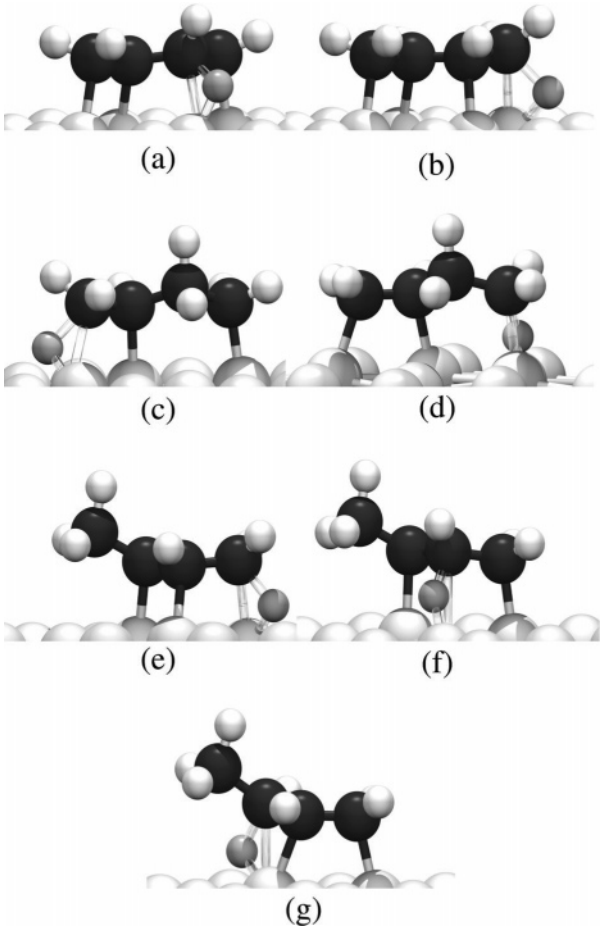

Figure 5. Transition state structures for the 1,3-butadiene hydrogenation on Pd(111): 13BD to 1B4R (a), 13BD to 2B1R (b), 1B4R to B13R (c), 1B4R to 1B (d), 2B1R to 2B (e), 2B1R to B13R (f), 2B1R to 1B(g). The reactive H atom is drawn in gray.

2-buten-1-yl is the most stable one (99 kJ mol^{-1}). This diradical species may continue to hydrogenate, explaining the primary formation of butane observed on platinum surfaces.[15]

We characterized the reaction pathways (Figure 4) on Pd(111) in parallel. The transition state structures for 1,3-butadiene hydrogenation on Pd have some strong similarities with those obtained on the Pt surface (see Figure 5a−g and Table 2), though some great energetic differences were found. In all the studied cases, the basic structure of the transition state is again a three-center cyclic intermediate (Pd−C−H). For the first hydrogenation step, the TSs to the monoradical intermediates are similar to those for Pt(111); see Figure 5a,b. Nevertheless, this first hydrogenation step is more endothermic and the energy difference between these two transition states is 36 kJ mol^{-1} (Figure 4). Obviously, the pathway via the 2-buten-1-yl (intrinsic barrier, 78 kJ mol^{-1}) intermediate seems to be favored with respect to the one through the 1-buten-4-yl (intrinsic barrier, 115 kJ mol^{-1}). This considerable difference can be ascribed to the poorer stability of the 1-buten-4-yl intermediate on the Pd(111) surface. As a result of the larger endothermicity, the transitions states are more product-like, i.e., later in the case of Pd.

The same trends found for the first hydrogenation were obtained for the second stage. The structures of the transition states are analogous to the ones obtained on Pt (see Figure 3c−g and Figure 5c−g, for comparison). The main differences involve the saddle point energies. It is clear that the paths leading to the butene isomers (especially to 1-butene) are quite favored on the palladium surface with respect to those leading to diradicals. The minimum energy profile occurs via the 2-buten-1-yl intermediate and leads to the 1-butene molecule with an overall barrier of 120 kJ mol^{-1}. The path to the 2-butene species requires 14 kJ mol^{-1} more to overcome the second hydrogenation barrier. Although one can consider that hydrogenation to the *cis*-2-butene species is similar to the reaction leading to the *trans* isomer, the *trans/cis* ratio observed experimentally is high. The clear difference has been ascribed to the low conformational interconversion of adsorbed species.[4] Both transition states leading to the butan-1,3-diyl radical are less stable by 39−55 kJ mol^{-1} with respect to the most stable one leading to 1-butene. This difference is large enough to be conclusive even if we take into account the possible errors arising from the DFT approach. One can also notice that on Pd(111) the transition states to form the butan-1,3-diyl diradical are later than on Pt(111), mainly due to the poor stability of the final product. Hence on the Pd(111) surface the formation of the diradical species seems totally unlikely, in clear contrast with the case of Pt(111). Therefore, no alternative path to obtain butane is possible, and it can be obtained only by subsequent hydrogenation of butene species formed as an initial product.

Analysis

It seems clear that the key of the selectivity to butene or butane rests on the relative stability of the butan-1,3-diyl intermediate species on Pt(111) and Pd(111). The adsorption

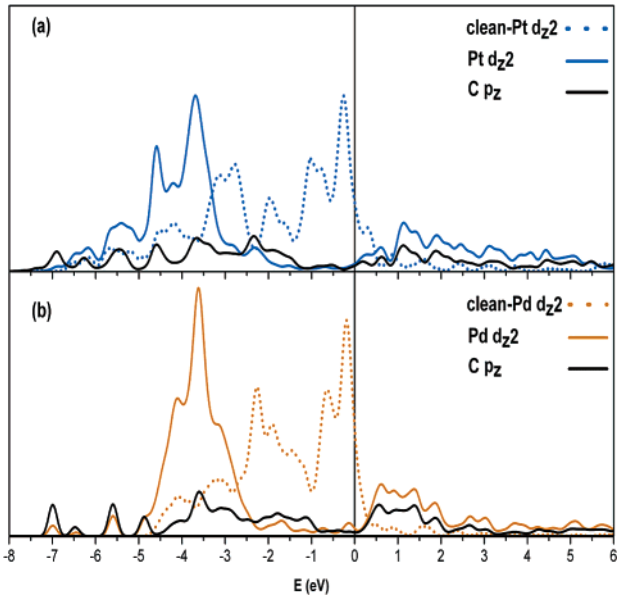

Figure 6. Projected density of states (PDOS) for butan-1,3-diyl on Pt(111) (a) and Pd(111) (b).

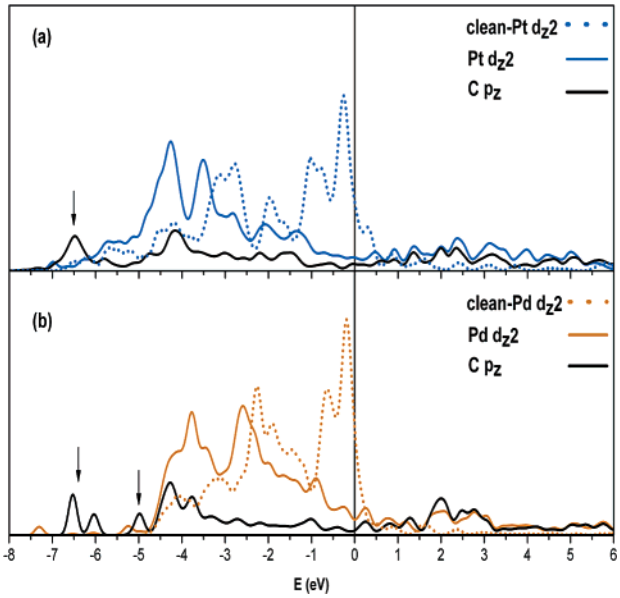

Figure 7. Projected density of states (PDOS) for 1-butene on Pt(111) (a) and Pd(111) (b). Arrows show the peaks resulting from the interaction of the Cp_z orbital with the Md_{xz} and Md_{yz}.

energy of the butan-1,3-diyl radical with respect to the diradical in the gas phase is −365 kJ mol^{-1} on Pt(111) and −326 kJ mol^{-1} on Pd(111). The diradical is very reactive and efficiently stabilized by chemisorption, but this effect is clearly stronger on the Pt(111) surface. For the 1-butene molecules the adsorption energy is −96 and −87 kJ mol^{-1} on Pt and Pd, respectively.

The analysis and comparison of the projected density of states (PDOS) curves (see Figures 6 and 7) can help us to understand these differences. The diradical intermediate adsorbs on both metal surfaces to form a five-atom metallacycle structure. In this adsorption mode, the carbon atoms directly point to a surface metal atom. Therefore, the interacting orbitals are mainly d_{z^2} for the metal atoms and p_z for the carbon. Upon formation of the M−C bond, there is a strong splitting of the d_{z^2} band (see Figure 6): the occupied part of the band is pushed downward and the empty part appears above the Fermi level (taken as energy zero) from the bonding and antibonding mixing with Cp_z. The d-band center below the Fermi level is placed at −4.08 eV and −3.56 eV for platinum and palladium, respectively. Above the Fermi level the d-band center is located at 2.49 eV (2.17 eV) for the Pt (Pd) surface. Obviously, these values yield a larger splitting in the case of Pt(111), 6.57 eV, compared with Pd, 5.73 eV. This result is consistent with the higher stability of the diradical species on Pt(111) compared with Pd(111). Two reasons can explain this difference: first, the smaller 4d orbital expansion of Pd, as seen from the narrower d-band in bulk, leads to a smaller surface−molecule overlap; second, the higher energy of the d states for Pd (more electropositive metal) increases the energy difference between them and Cp_z, which decreases the interaction.

The picture for butene species is quite similar. The interaction primarily takes place between the p_z orbital of the C atom and the d_{z^2} band of the metal atom (see PDOS, Figure 7). However, there is a non-negligible contribution of both d_{xz} and d_{yz} (peaks marked with an arrow in the PDOS curves arise from these interactions, Figure 7). The C_1C_2 bond is situated parallel above a metal−metal bond, allowing a better overlap between the Cp_z and these bands. A considerable splitting of the d_{z^2} band is observed upon adsorption of the butene molecule, though it is not as strong as with the diradical adsorption. Again the energy difference between the center of the d_{z^2} band below and over the Fermi level is bigger on the platinum surface (by 0.9 eV). The electronic interaction is therefore again more important on Pt than on Pd. However, the adsorption energy of 1-butene on Pt(111) and Pd(111) differs only by 9 kJ mol^{-1}, to be compared with the 39 kJ mol^{-1} difference obtained for the diradical.

The decomposition of the adsorption energy in its main contributions has been performed in order to explain the differences obtained.[26] The adsorption energy is partitioned into three contributions: distortion energy of the molecule, distortion energy of the surface, and adsorbate−substrate interaction energy where the molecular fragment and the surface are kept in the geometry of the adsorbed system. In the case of the butan-1,3-diyl radical, the difference in distortion energy of the species and the surface on both metal surfaces is less than 9 kJ mol^{-1}. Consequently, the difference in adsorption energy arises from the interaction energy part between the diradical and the surface (−434 kJ mol^{-1} on Pt, compared with −380 kJ mol^{-1} on Pd). For 1-butene, the energy costs to distort the molecule from its geometry in the gas phase to its adsorption geometry is 51 kJ mol^{-1} less on Pd(111). The higher distortion energy on Pt is consistent with the stronger hybridization and the greater elongation of the C_1-C_2 bond upon adsorption (see Table 1). As the distortion energy of the surface is similar for both surfaces, the interaction energy is 66 kJ mol^{-1} stronger on platinum than on palladium (−260 vs −194 kJ mol^{-1} on Pt and Pd, respectively). This fact is also noticeable in the PDOS curve (Figure 7), the broadening of the Cp_z states being more important on Pt than on Pd.

Conclusion

The natural chemical pathway to hydrogenate butadiene is to conserve a double bond by forming butene (1-butene from 1−2 attack or 2-butene by 1−4 attack). The 1−3 (or 2−4) attack leads to a diradical species, butan-1,3-diyl, which is very unstable in the gas phase. Our calculations show that this diradical is strongly stabilized by the interaction with the catalytic surface (especially on the Pt(111) surface).

The pathway toward the butan-1,3-diyl radical becomes competitive with those leading to butenes in the case of the Pt catalyst. The transformation (1,3-butadiene (13BD) → 2-buten-

1-yl (2B1R) → butan-1,3-diyl (B13R)) is indeed associated with the lowest activation barrier (99 kJ mol^{-1}), but the pathway to 1-butene (1,3-butadiene (13BD) → 2-buten-1-yl (2B1R) → 1-butene (1B)) is only 7 kJ mol^{-1} higher. From the typical error bars in such calculations, it is possible to conclude here only that these two pathways are equally probable. The formed butene will desorb as long as butadiene is present in the gas phase since the adsorption of butadiene is strongly favored. The diradical species will be further hydrogenated, leading to the formation of butane as primary product and to an incomplete selectivity to butene. This is in good agreement with the partial selectivity (60%) to butene observed on Pt(111) and with the presence of butane right from the beginning of the reaction.

Although the butan-1,3-diyl is also stabilized on Pd(111), this effect is smaller than on Pt(111) and the pathway toward this radical is not accessible, with a transition state 39 kJ mol^{-1} less stable than that of 1-butene. Taking into account all possible sources of error, this energy difference is large enough to categorically exclude this transformation (1,3-butadiene (13BD) → 2-buten-1-yl (2B1R) → butan-1,3-diyl (B13R)) on Pd(111). Calculations hence predict a full selectivity to butene in agreement with the experiment.

Moreover, the pathway to 1-butene has a lower activation energy than the one to 2-butene on both metals, in agreement with the observed distribution of products.

The smaller stabilization of the 1−3 diradical on Pd(111) compared to Pt(111) can be qualitatively explained by the analysis of the one-electron states and related to the smaller expansion of the 4d orbitals of Pd (vs 5d of Pt).

These results on the example of butadiene shed light on the factors that control activity and selectivity of a catalyst. It is well known that the key role of a catalyst is to stabilize unstable gas phase species, such as intermediates or transition states, to allow a lower energy profile transformation. Here, the key step is to stabilize the monohydrogenated intermediates 1-buten-4-yl and 2-buten-1-yl radicals. However by the same mechanism, the catalyst can also stabilize the diradical isomers of the butene product. A selective reaction implies that the consecutive elementary steps must occur in a controlled way. Otherwise, the occurrence of side reactions leads to a poor selectivity. Therefore, an optimum catalyst for the 1,3-butadiene hydrogenation must reach a compromise between the stabilization of key intermediates and transition states and the strength of chemisorption of the unwanted diradical intermediates.

These results can be directly extended to the selective hydrogenation of other conjugated organic molecules, such as benzene. Moreover, calculations also open ideas to improve the Pt catalyst. It could be envisaged to hinder the adsorption of the diradical species by modifying the monometallic catalyst via addition of a second metal.

Acknowledgment. The authors thank the Institut du Développement et des Ressources en Informatique Scientifique (IDRIS) at Orsay (project 609) and the Centre Informatique National de l'Enseignement Supérieur (CINES) at Montpelier for CPU time. A.V. acknowledges financial support through the TMR activity "Marie Curie research training grants". Funding from the Spanish Ministerio de Ciencia y Tecnología (BQU2002-04029-CO2-02) and the Catalan Government (2001SGR00315) is also acknowledged.

References and Notes

(1) Cosyns, J. *Catalyse par les Métaux*; Imelik, B., Martin, G. A., Renouprez, A. J., Eds.; CNRS: Paris, 1984; p 371.
(2) Massadier, J.; Bertolini, J. C.; Renouprez, A. *Proceedings of the 9th International Congress on Catalysis*; Calgary, Phillips, M. J., Ternan, M., Eds.; 1988; Vol. III, p 1222.
(3) Ouchaib, T.; Massadier, J.; Renouprez, A. *J. Catal.* **1989**, *119*, 517.
(4) Goetz, J.; Murzin, D. Y.; Touroude, R. A. *Ind. Eng. Chem. Res.* **1996**, *35*, 703.
(5) Yoon, C.; Yang, M. X.; Somorjai, G. A. *Catal. Lett.* **1997**, *46*, 37.
(6) Tourillon, G.; Cassuto, A.; Jugnet, Y.; Massadier, J.; Bertolini, J. C. *J. Chem. Soc., Faraday Trans.* **1996**, *92*, 4835.
(7) Pradier, C.-M.; Margot, E.; Berthier, Y.; Oudar, J. *Appl. Catal.* **1988**, *43*, 177.
(8) Abon, M.; Bertolini, J. C.; Tardy, B. *J. Chim. Phys.* **1988**, *85*, 711.
(9) Bertolini, J. C.; Cassuto, A.; Jugnet, Y.; Massardier, J.; Tardy, B.; Tourillon, G. *Surf. Sci.* **1996**, *349*, 88.
(10) Maurice, V.; Minot, C. *Langmuir* **1989**, *5*, 734.
(11) Sautet, P.; Paul, J.-F. *Catal. Lett.* **1991**, *9*, 245.
(12) Bond G. C. *Catalysis by Metals*; Academic Press: London, 1962.
(13) McGrown, W. T.; Kemball, C.; Whan, D. *J. Catal.* **1978**, *51*, 173.
(14) Valcárcel, A.; Clotet, A.; Ricart, J. M.; Delbecq, F.; Sautet, P. *Surf. Sci.* **2004**, *549*, 121.
(15) Boitiaux, J. P.; Cosyns, J.; Robert, E. *Appl. Catal.* **1987**, *35*, 193.
(16) Bent, B. E.; Nuzzo, R. G.; Zegarski, B. R.; Dubois, L. H. *J. Am. Chem. Soc.* **1991**, *113*, 1143.
(17) Scoggins, T. B.; White, J. M. *J. Phys. Chem. B* **1997**, *101*, 7958.
(18) Chrysostomou, D.; Chou, A.; Zaera, F. *J. Phys. Chem. B* **2001**, *105*, 5968.
(19) Horiuti, I.; Polanyi, M. *J. Mol. Catal. A* **2003**, *199*, 185.
(20) Kresse, G.; Hafner, J. *Phys. Rev. B* **1993**, *47*, 558.
(21) Kresse, G.; Hafner, J. *Phys. Rev. B* **1993**, *48*, 13115.
(22) Kresse, G.; Hafner, J. *Phys. Rev. B* **1994**, *49*, 14251.
(23) Blöchl, P. *Phys. Rev. B* **1994**, *50*, 17953.
(24) Kresse, G.; Joubert, D. *Phys. Rev. B* **1998**, *59*, 1758.
(25) Perdew, J. P.; Wang, Y. *Phys. Rev. B* **1992**, *45*, 13244.
(26) Morin, C.; Simon, D.; Sautet, P. *J. Phys. Chem. B* **2003**, *107*, 2995.
(27) Wyckoff, R. W. G. *Crystal Structures*, 2nd ed.; Interscience: New York, 1965; Vol. 1.
(28) Jónsson, H.; Mills, G.; Jacobsen, K. W. *Classical and Quantum Dynamics in Condensed Phase Simulations*; Berne, J. B., Ciccotti, G., Coker, D. F., Eds.; World Scientific: Singapore, 1998; p 385.
(29) Henkelman, G.; Jónsson, H. *J. Chem. Phys.* **1999**, *111*, 7010.
(30) Légaré, P. *Surf. Sci.* **2004**, *559*, 169.
(31) Neurock, M.; van Santen, R. A. *J. Phys. Chem. B* **2000**, *104*, 11127.
(32) Sheth, P. A.; Neurock, M.; Smith, C. M. *J. Phys. Chem. B* **2003**, *107*, 2009.
(33) Koga, N.; Jin, S. Q.; Morokuma, K. *J. Am. Chem. Soc.* **1988**, *110*, 3417.